

# Unidirectional spin transport of a spin-orbit-coupled atomic matter wave using a moving Dirac $\delta$ -potential well

Jieli Qin<sup>1,\*</sup> and Lu Zhou<sup>2,3,†</sup>

<sup>1</sup>*School of Physics and Electronic Engineering, Guangzhou University, 230 Wai Huan Xi Road, Guangzhou Higher Education Mega Center, Guangzhou 510006, People's Republic of China*

<sup>2</sup>*Department of Physics, School of Physics and Electronic Science, East China Normal University, Shanghai 200241, People's Republic of China*

<sup>3</sup>*Collaborative Innovation Center of Extreme Optics, Shanxi University, Taiyuan, Shanxi 030006, People's Republic of China*

We study the transport of a spin-orbit-coupled atomic matter wave using a moving Dirac  $\delta$ -potential well. In a spin-orbit-coupled system, bound states can be formed in both ground and excited energy levels with a Dirac  $\delta$ -potential. Because Galilean invariance is broken in a spin-orbit-coupled system, moving of the potential will induce a velocity-dependent effective detuning. This induced detuning breaks the spin symmetry and makes the ground-state transporting channel be spin- $\uparrow$  ( $\downarrow$ ) favored while makes the excited state transporting channel be spin- $\downarrow$  ( $\uparrow$ ) favored for a positive-direction (negative-direction) transporting. When the  $\delta$ -potential well moves at a small velocity, both the ground-state and excited-state channels contribute to the transportation, and thus both the spin components can be efficiently transported. However, when the moving velocity of the  $\delta$ -potential well exceeds a critical value, the induced detuning is large enough to eliminate the excited bound state, and makes the ground bound state the only transporting channel, in which only the spin- $\uparrow$  ( $\downarrow$ ) component can be efficiently transported in a positive (negative) direction. This work demonstrates a prototype of unidirectional spin transport.

## I. INTRODUCTION

Transport of matterwave is essential in many ultracold atom physics experiments and applications. With such a technique, an ultracold atom experiment can be split into matterwave producing and matterwave using modules. Each module can be optimized separately. Thus the experiment can be performed more efficiently [1–3]. In this thought, for example, atomic gases have been loaded into optical cavities [4–9] and hollow fibers [10–14], leading to a good many interesting research works (for reviews see references [15–17]). It is also found that the transport of atomic matterwave can be very useful in the realization of atom interferometry [18–20], atomtronics device [21–24] and continuous atom laser [25–27].

Many schemes to transport cold atomic matterwave have been demonstrated. In moving molasses technique [28, 29], the cloud of cold atoms freely flies to the destination by itself. Controlled transport can be realized by applying an atomic waveguide [30–40]. However, using these techniques, the cloud of atoms expands, and its density drops during the transporting process. To overcome this blemish, matterwave transport using a moving potential well is introduced, and soon becomes widely used in cold atom experiments [1–3, 26, 41–46].

The moving dynamic of spin-orbit (SO) coupled matterwave shows new features. For a SO coupled system, the Galilean invariance does not hold any more [47–49]. Different moving directions or speeds can have very

different effects on the dynamics of SO coupled atomic gases. As a result, many interesting phenomena arise. A few examples are listed below. The critical velocity of superfluidity becomes reference frame dependent [50]. An oscillation of magnetization in SO coupled Bose-Einstein condensate (BEC) is induced by the moving [51, 52]. The shape of a SO coupled BEC bright soliton changes with its velocity [53]. In a translating optical lattice, SO coupled BEC behaves anisotropically depending on the direction of translation [54]. The normal density of superfluidity does not vanish even at zero temperature [55]. And, non-magnetic one-way spin switch [56] and spin-current generation [57] have also been demonstrated recently.

In this paper, we study the transport of SO coupled cold atomic matterwave using a moving Dirac delta-potential well, see diagram figure 1. We show that the delta-potential well can at most support both a ground and an excited bound state in SO coupled cold atom system. These bound states can be used to efficiently transport the cold atomic matterwave, thus serve as the transporting channels in the problem. Moving of the potential well will induce a velocity proportional effective detuning, which can substantially affect the transporting channels. This induced detuning breaks the spin symmetry, and makes the two transporting channels being spin-polarized. For a slowly positive direction moving delta-potential well, the ground state channel is spin- $\uparrow$  favored, while the excited state channel is spin- $\downarrow$  favored. Both the spin- $\uparrow$  and spin- $\downarrow$  components can be transported through its favorable channel. And for a slowly negative direction moving delta-potential well, things are very similar, except that the roles of spin- $\uparrow$  and spin- $\downarrow$  exchange with each other. When the velocity of the

\* 104531@gzhu.edu.cn; qinjieli@126.com

† lzhou@phy.ecnu.edu.cn

moving delta-potential well exceeds a critical value, the induced effective detuning will be large enough to lift the excited state out of the binding ability of the delta-potential well, thus eliminate the excited bound state transporting channel. Therefore, in such a case, matter-wave can only be transported through the ground state channel. Since for a positive (negative) direction moving delta-potential well, the ground state channel is spin- $\uparrow$  (spin- $\downarrow$ ) dominant, only this appropriate spin component of matterwave can be efficiently transported. These unidirectional transporting features indicate that the system considered here may potentially be used to realize spintronic devices such as spin diode [58, 59], valve [60] and filter [61, 62].

The rest part of this paper is organized as follows: In section II, the physical model of this paper is presented. In section III, we solve the bound states (i.e., the transporting channels) of the moving delta-potential well, and discuss their properties. In section IV, the transporting dynamics and efficiency are shown. And at last, the paper is summarized in section V.

## II. MODEL

We consider the transporting of quasi-one-dimensional SO coupled cold atoms using a moving delta-potential well, see figure 1. The SO coupling is realized by the two x-direction counter-propagating Raman lasers  $L_1$  and  $L_2$  [63]. And the delta-potential well can be generated using a y-direction shining tightly focused laser beam [64, 65]. Such a system can be described by Hamiltonian

$$H = H_0 + U(x, t), \quad (1)$$

where  $U(x, t)$  is the external potential, and  $H_0$  is the SO coupled free particle Hamiltonian

$$H_0 = \begin{bmatrix} \frac{(p_x - p_c)^2}{2m} - \frac{\hbar\Delta_0}{2} & \frac{\hbar\Omega}{2} \\ \frac{\hbar\Omega}{2} & \frac{(p_x + p_c)^2}{2m} + \frac{\hbar\Delta_0}{2} \end{bmatrix}. \quad (2)$$

Here  $p_x = \hbar k_x = -i\hbar \frac{\partial}{\partial x}$  is the one-dimensional momentum operator,  $p_c = \hbar k_c$  is the strength of SO coupling determined by momentum transfer during the Raman scattering process,  $\Delta_0$  is the detuning of the Raman driving from the atomic energy level splitting (in this paper we assume that its value is set to zero  $\Delta_0 = 0$ ),  $\Omega$  is the effective Rabi frequency for Raman flipping between the two spin states. The inter-atom collision interaction is not included here, as it is assumed to have been eliminated by the Feshbach resonance technique [66, 67]. In the following contents, for convenience natural unit  $\hbar = m = 1$  will be used.

Before time  $t = 0$ , the system is prepared in the ground state of a delta-potential well localized at  $x = 0$ . Then, for time  $t > 0$ , we move the delta-potential well at a constant velocity  $v$ , and study the subsequent transportation. Hence, the external potential  $U(x, t)$  can be written

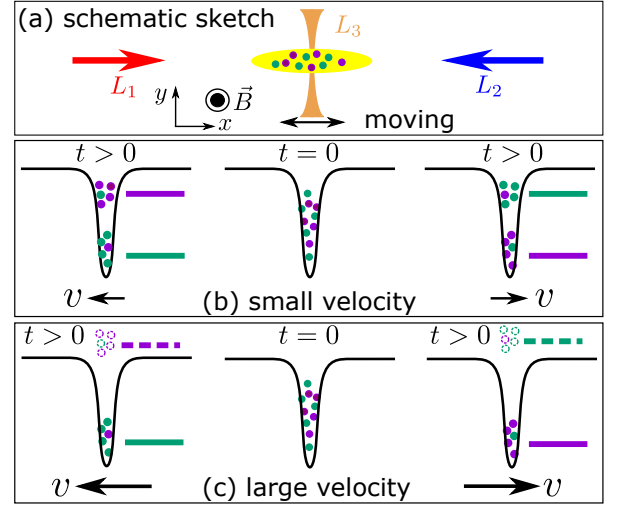


Figure 1. Diagram of transporting SO coupled cold atomic matterwave using a moving delta-potential well. At time  $t = 0$ , an atomic SO coupled BEC is prepared in the ground state of a delta-potential well. The atoms are equally distributed in the spin- $\uparrow$  and spin- $\downarrow$  components. Afterward, one moves the delta-potential well at velocity  $v$  to transport the matterwave. Top panel (a): Schematic sketch of the system. The SO coupling is realized by the two counter-propagating Raman lasers  $L_1$  and  $L_2$ . The third tightly focused movable laser beam  $L_3$  generates the delta-potential well. Middle panel (b): For a small velocity moving delta-potential well, it can support two transporting channels — ground and excited bound states of the moving delta-potential well in the comoving frame. One of the transporting channels is spin- $\uparrow$  favored, while the other one is spin- $\downarrow$  favored. Both the spin- $\uparrow$  and spin- $\downarrow$  components can be efficiently transported in such a case. Bottom panel (c): For a large velocity moving delta-potential well, the moving induced effective detuning lifts the excited state out of the binding ability of the potential well, thus matterwave transportation can only take place in the ground state channel. For a positive (negative) direction moving delta-potential well, the ground state channel is spin- $\uparrow$  (spin- $\downarrow$ ) dominant, thus only the spin- $\uparrow$  (spin- $\downarrow$ ) component can be efficiently transported.

in a piece-wise function as follows

$$U(x, t) = \begin{cases} V_0(x) = -V_0\delta(x), & t \leq 0, \\ V(x, t) = -V_0\delta(x - vt), & t > 0. \end{cases} \quad (3)$$

The initial state can be constructed using the free particle oscillating evanescent wave modes (for detail see section III)

$$\psi_0 = \begin{cases} A_{0,1}\xi_{-;1}e^{ik_{x;1}x} + A_{0,2}\xi_{-;2}e^{ik_{x;2}x}, & x \leq 0, \\ A_{0,3}\xi_{-;3}e^{ik_{x;3}x} + A_{0,4}\xi_{-;4}e^{ik_{x;4}x}, & x > 0. \end{cases} \quad (4)$$

The transporting dynamic for time  $t > 0$  is governed by time-dependent Schrödinger equation

$$i\frac{\partial\psi(x, t)}{\partial t} = H(x, t)\psi(x, t). \quad (5)$$

Noticed that here the Hamiltonian is time-dependent, it will be convenient to deal with the problem in a frame comoving with the potential. So we take the following transformation

$$x \rightarrow x - vt, \quad t \rightarrow t, \quad (6)$$

and

$$\psi \rightarrow \psi e^{-ivx} e^{iv^2 t/2}. \quad (7)$$

Under this transformation, equation (5) becomes

$$i \frac{\partial \psi(x, t)}{\partial t} = H_t \psi(x, t), \quad (8)$$

with the transformed Hamiltonian being [51]

$$H_t = \frac{1}{2} \begin{bmatrix} (k_x - k_c)^2 - \Delta & \Omega \\ \Omega & (k_x + k_c)^2 + \Delta \end{bmatrix} + V_0(x), \quad (9)$$

where

$$\Delta = 2k_c v, \quad (10)$$

is an effective detuning induced by the moving of external potential.

This new time-independent Hamiltonian is similar to the Hamiltonian at time  $t = 0$ , except for the moving induced additional detuning term. Therefore, the moving delta-potential also supports bound states, and these bound states can also be constructed similarly using the oscillating evanescent waves (for detail also see section III)

$$\psi_{tb} = \begin{cases} A_{t,1} \xi_{-;t1} e^{ik_{x;t1}x} + A_{t,2} \xi_{-;t2} e^{ik_{x;t2}x}, & x \leq 0, \\ A_{t,3} \xi_{-;t3} e^{ik_{x;t3}x} + A_{t,4} \xi_{-;t4} e^{ik_{x;t4}x}, & x > 0. \end{cases} \quad (11)$$

These states are bounded by, and at the same time, comove with the external potential, thus can serve as the transporting channels of the system. In the next section, we will show that the moving delta-potential well can at most support two bound states. We label them as  $\psi_{tb;g}$  and  $\psi_{tb;e}$ , with subscript “ $g$ ” and “ $e$ ” meaning the ground and excited states. And, the excited state disappears for large potential moving velocity. Hamiltonian (9) also supports an infinite number of scattering states. However, after a long-time evolution, these states spread all over the whole space and have negligible densities. Therefore, they are not important for the transportation. Neglecting them, the efficiently transported matterwave can be described by the following wavefunction [68, 69]

$$\psi_t = C_g \psi_{tb;g} e^{-iE_g t} + C_e \psi_{tb;e} e^{-iE_e t}, \quad (12)$$

where  $E_g$  and  $E_e$  are the ground state and excited state eigenenergies, and  $C_g$  and  $C_e$  are the ground state and

excited state probability amplitudes determined by the initial wavefunction according to formulae

$$C_{g,e} = \int_{-\infty}^{\infty} \psi_{tb;g,e}^\dagger \psi_0 e^{ivx} dx. \quad (13)$$

Here, when the excited state does not exist, one simply sets  $C_e = 0$  to eliminate its role.

At last, we define some quantities to characterize the transporting efficiency of the moving delta-potential well. The time averaged spin- $\uparrow$  and spin- $\downarrow$  atom numbers of transported matterwave are given by

$$N_{t;\uparrow,\downarrow} = \sum_{i=g,e} \int |C_i \psi_{tb;i\uparrow,\downarrow}|^2 dx, \quad (14)$$

And the time averaged total atom number of transported matterwave is

$$N_t = N_{t;\uparrow} + N_{t;\downarrow} = |C_g|^2 + |C_e|^2. \quad (15)$$

We emphasize that the total atom number of initial state  $\psi_0$  will be normalized to 1 in this paper, therefore  $N_{t;\uparrow,\downarrow}$  and  $N_t$  defined here indeed can be interpreted as the fraction of transported atoms compared to the initial state.

### III. TRANSPORTING CHANNELS: BOUND STATES OF THE MOVING DELTA-POTENTIAL WELL

From the previous section, one sees that both the initial state and transporting channel problems involve finding the bound eigenstates of SO coupled cold atomic matterwave. For a delta-potential well  $V_0(x) = -V_0 \delta(x)$ , it is equivalent to a free space problem except for the very point  $x = 0$ . So the bound eigenstates of a delta-potential well can be constructed using the free particle modes by matching boundary conditions at  $x = 0$  [70]. In this section, we first discuss the free particle spectrum and eigenstates of a SO coupled system, and then construct the bound states using the free particle modes.

The free particle modes can be found by diagonalizing Hamiltonian (9) (with  $V_0(x)$  neglected). It comes out that the eigenenergy is given by

$$\left[ E - \frac{(k_x^2 + k_c^2)}{2} \right]^2 - \left( k_c k_x + \frac{\Delta}{2} \right)^2 + \left( \frac{\Omega}{2} \right)^2 = 0, \quad (16)$$

which is a second-order equation of  $E$ . This indicates that the spectrum will split into two branches (we recognize them as “lower” and “upper” branch in this paper)

$$E_{\pm} = \frac{k_x^2 + k_c^2}{2} \pm \frac{1}{2} \sqrt{(2k_c k_x + \Delta)^2 + \Omega^2}, \quad (17)$$

and the corresponding eigenstates are

$$\psi_{\pm}(k_x) = \xi_{\pm}(k_x) e^{ik_x x} = C_{\pm} \begin{pmatrix} \zeta_{\pm} \\ 1 \end{pmatrix} e^{ik_x x}, \quad (18)$$

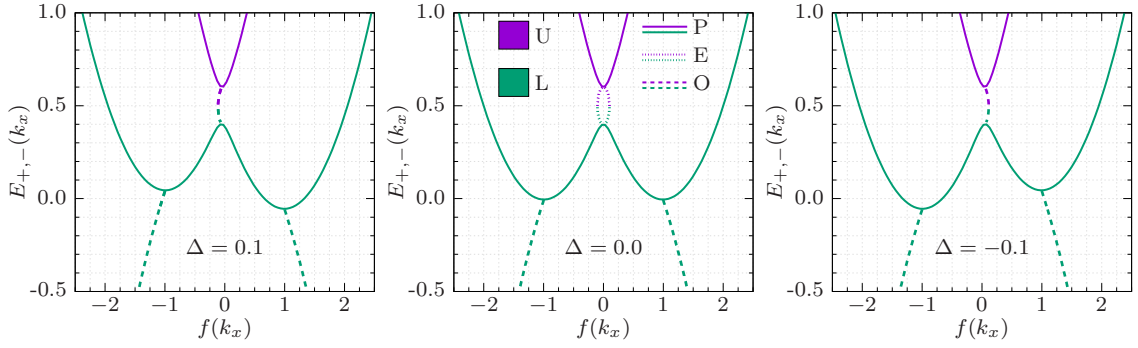


Figure 2. Free particle spectrum of SO coupled cold atomic matterwave. SO coupling and Rabi coupling strengths are  $k_c = 1, \Omega = 0.2$ . Left panel: positive detuning  $\Delta = 0.1$ . Middle panel: zero detuning  $\Delta = 0$ . Right panel: negative detuning  $\Delta = -0.1$ . The violet lines correspond to the upper (“U”) spectrum branch  $E_+$ , while the green lines correspond to the lower (“L”) spectrum branch  $E_-$ . The solid, dashed and dotted lines represent plane traveling (“P”), oscillating evanescent (“O”) and ordinary evanescent (“E”) waves, respectively. For plane traveling wave, wavevector  $k_x$  has a real number value, the  $x$ -axis is set to  $f(k_x) = k_x$ ; for oscillating evanescent wave,  $k_x = \beta \pm i\alpha$ , the  $x$ -axis is set to  $f(k_x) = \text{sgn}[\text{Re}(k_x)] \cdot |k_x|$  (therefore, the lines for  $+\alpha$  and  $-\alpha$  overlap with each other); and for ordinary evanescent wave,  $k_x = \pm i\alpha$ , the  $x$ -axis is set to  $f(k_x) = \text{sgn}[\text{Im}(k_x)] \cdot |k_x|$ .

where  $\zeta_{\pm} = -(2k_c k_x + \Delta) / \Omega \pm \sqrt{(2k_c k_x + \Delta)^2 / \Omega^2 + 1}$  characterize the spin wavefunction, and  $C_{\pm} = 1 / \sqrt{1 + |\zeta_{\pm}|^2}$  is the normalization parameter.

Equation (16) admits three kinds of wavevectors with real, pure imaginary and complex value, respectively. The real part of wavevector  $k_x$  contributes a plane traveling wave factor in the eigenstate (18), while the imaginary value part contributes an exponential decay factor. Thus, corresponding to these three kinds of wavevectors, the eigenstates are plane traveling wave, ordinary evanescent wave, and oscillating evanescent wave states, respectively [71, 72]. For different strengths of SO coupling  $k_c$  and Rabi coupling  $\Omega$ , the spectrum of the system can be a little different. Here we focus on the strong SO coupling case with  $k_c > \Omega/2$ , and numerically we choose  $k_c = 1$  and  $\Omega = 0.2$  all over the paper. In figure 2, the free particle spectra are plotted for different detunings  $\Delta = 0, \pm 0.1$ . In the figure, different types of eigenstates are marked with different styles of lines. From the figure, one sees that for energy below the minimum of lower branch spectrum  $E_0 < E_{-,min}$ , the four eigenmodes are all oscillating evanescent waves. Further calculations show that the corresponding wavevectors, i.e., solutions of equation (16), have the following symmetric form

$$k_{x;1,3} = \beta \mp i\alpha_I, \quad k_{x;2,4} = -\beta \mp i\alpha_{II}. \quad (19)$$

Here  $\alpha_{I,II}$  and  $\beta$  are real positive numbers. Specially, when  $\Delta = 0$ , the two imaginary part numbers also equal each other  $\alpha_I = \alpha_{II} = \alpha$ .

Since waves  $\exp[ik_{x;1,2}] = \exp[\pm i\beta x + \alpha_{I,II} x]$  decay to zero when  $x \rightarrow -\infty$ , while waves  $\exp[ik_{x;3,4}] = \exp[\pm i\beta x - \alpha_{I,II} x]$  decay to zero when  $x \rightarrow +\infty$ , the bound states of a delta-potential well can be constructed using these four oscillating evanescent wave modes. The

wave function can be written as

$$\begin{aligned} \psi_b &= \begin{cases} A_1 \xi_{-,1} e^{ik_{x;1} x} + A_2 \xi_{-,2} e^{ik_{x;2} x}, & x < 0, \\ A_3 \xi_{-,3} e^{ik_{x;3} x} + A_4 \xi_{-,4} e^{ik_{x;4} x}, & x > 0, \end{cases} \\ &= \begin{cases} A_1 \xi_{-,1} e^{i\beta x + \alpha_I x} + A_2 \xi_{-,2} e^{-i\beta x + \alpha_{II} x}, & x < 0, \\ A_3 \xi_{-,3} e^{i\beta x - \alpha_I x} + A_4 \xi_{-,4} e^{-i\beta x - \alpha_{II} x}, & x > 0, \end{cases} \end{aligned} \quad (20)$$

with symbols  $\xi_{-,1,2,3,4} = \xi_{-}(k_{x;1,2,3,4})$  for shorthand. The wavefunction parameters  $A_{1,2,3,4}$  and eigenenergy  $E_b(k_{x;1,2,3,4})$  are determined by  $E_b$  according to equation (16) are to be determined by normalization constrain  $\int_{-\infty}^{\infty} |\psi_b|^2 dx = 1$  together with boundary conditions: continuity of wavefunction

$$\psi_b(x)|_{0+} = \psi_b(x)|_{0-}, \quad (21)$$

and jump of the first-order derivative of wave function caused by the singularity of delta-potential

$$\left. \frac{d\psi_b(x)}{dx} \right|_{0+} - \left. \frac{d\psi_b(x)}{dx} \right|_{0-} = -2V_0 \psi_b(x=0). \quad (22)$$

Because of the spin-1/2 nature of the system, a delta-potential well can support two bound states (which are recognized as ground and excited states in this paper) with spin symmetry  $|\psi_{\downarrow}|^2 = |\psi_{\uparrow}|^2$  when the detuning is absent ( $\Delta = 0$ ). When a small detuning is introduced, this spin symmetry is broken,  $|\psi_{\downarrow}|^2 \neq |\psi_{\uparrow}|^2$ . According to the Hamiltonian (1), a positive detuning will raise the energy of spin- $\downarrow$  (or in other words, negative momentum) component, and at the same time, lower the energy of spin- $\uparrow$  (negative momentum) component. This fact can also be seen from the spectrum shown in figure 2. As a result, the ground state becomes spin- $\uparrow$  favored, while the excited state becomes spin- $\downarrow$  favored. When the detuning becomes large, the energy of the excited state will



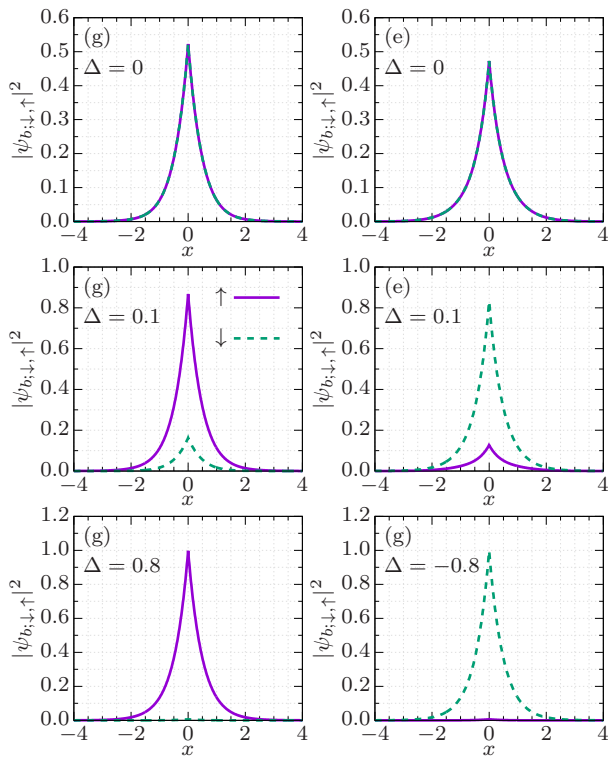


Figure 3. Eigenstates of delta-potential well trapped SO coupled cold atomic matterwave for different effective detunings ( $\Delta = 2k_c v = 0, 0.1, \pm 0.8$ ). The solid violet lines stand for spin- $\uparrow$  component atomic density  $|\psi_{b;\uparrow}|^2$ , while the green dashed lines stand for spin- $\downarrow$  component atomic density  $|\psi_{b;\downarrow}|^2$ . Top panels: spin symmetric ground (“g”) and excited (“e”) states for zero detuning  $\Delta = 0$ . Middle panels: spin asymmetric ground and excited states for a small detuning  $\Delta = 0.1$ . Bottom panels: spin asymmetric ground states for large positive  $\Delta = 0.8$  and negative detuning  $\Delta = -0.8$ . The excited state is absent for such large detunings, thus only the ground state is plotted. The eigenenergies corresponding to these states are  $-0.5536, -0.4540, -0.5742, -0.4334, -0.9056, -0.9056$ , respectively. The SO coupling and Rabi coupling strengths are  $k_c = 1, \Omega = 0.2$ , and the depth of the delta-potential well is  $V_0 = 1$ .

be raised out of the binding ability of the potential well, hence the excited state disappears. For a negative detuning, the roles of spin- $\uparrow$  and spin- $\downarrow$  exchange with each other. These facts are shown in figure 3, where ground and excited bound states are plotted for zero and small detunings  $\Delta = 0, 0.1$ . And for large detunings  $\Delta = \pm 0.8$ , the excited state disappears, only the ground state is plotted.

We also studied the delta-potential well bounded SO coupled spectrum. The ground state and excited state energies are plotted as a function of detuning  $\Delta$  in figure 4. The detuning induced energy splitting of the two states, and the disappearing of the excited state can be clearly seen in this figure. And one also noticed that for a deeper potential well the excited state disappears at a larger value of detuning  $\Delta$ . This is further shown

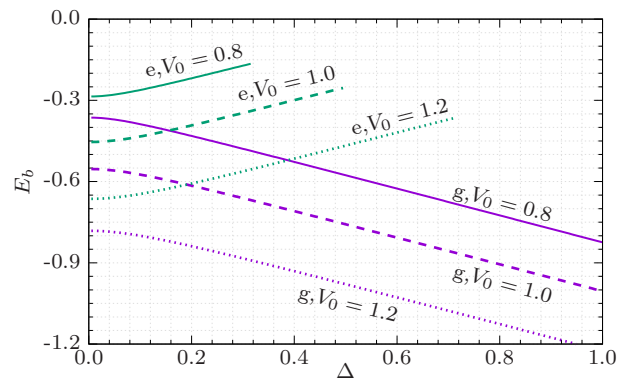


Figure 4. The spectrum of delta-potential bounded SO coupled cold atomic matterwave. Ground (“g”, violet lines) and excited (“e”, green lines) state energies  $E_{b;g,e}$  are plotted as a function of effective detuning  $\Delta = 2k_c v$ . Solid, dashed and dotted lines represent different potential well depths  $V_0 = 0.8, 1.0, 1.2$ , respectively. SO coupling strength and Rabi frequency are  $k_c = 1, \Omega = 0.2$ .

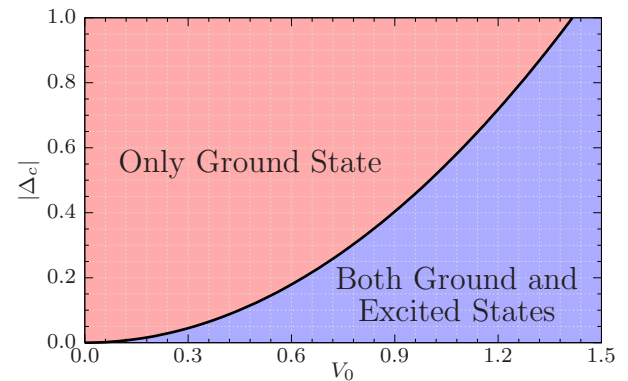


Figure 5. Critical detuning for the disappearing of the excited state. The absolute value of critical detuning is plotted as a function of delta-potential well depth  $V_0$ , the black solid line. Below this line, the light blue color filled region supports both a ground and an excited bound state. While above this line, the pink color filled region supports only one bound state, the ground state. SO coupling strength and Rabi frequency are  $k_c = 1, \Omega = 0.2$ .

in figure 5, where the excited state disappearing critical detuning  $\Delta_c$  is plotted as a function of delta-potential well depth  $V_0$ . In this figure, in the region below the critical-value-line (the black solid line), both the ground and excited states exist, while above the line the excited state disappears, and there is only one bound state, the ground state.

At last, recalling that moving can induce an effective detuning  $\Delta = 2k_c v$ , it is concluded that a small positive (negative) velocity moving delta-potential well can support both a spin- $\uparrow$  (spin- $\downarrow$ ) favored ground state and a spin- $\downarrow$  (spin- $\uparrow$ ) favored excited state transporting channel, while a large positive (negative) velocity moving delta-potential well can only support a spin- $\uparrow$  (spin- $\downarrow$ ) dominant ground state transporting channel. This will

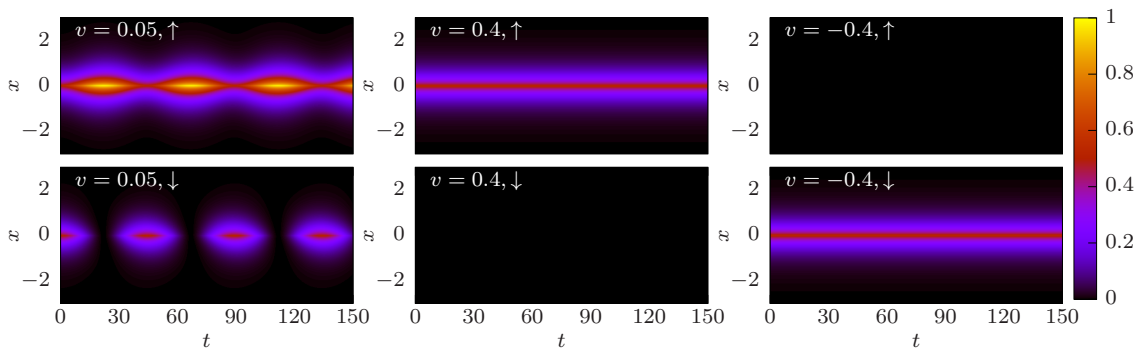


Figure 6. Time evolution of the transported matterwave under different potential moving velocities. Left panel: Interference pattern between the ground state and excited state channels transported matterwave for a small velocity ( $v = 0.05$ ) moving delta-potential well. Middle panel: Spin- $\uparrow$  component dominant transporting for a large velocity positive direction moving ( $v = 0.4$ ) delta-potential well. Right panel: Spin- $\downarrow$  component dominant transporting for a large velocity negative direction moving ( $v = -0.4$ ) delta-potential well. SO coupling strength, Rabi frequency and depth of the delta-potential well are  $k_c = 1$ ,  $\Omega = 0.2$  and  $V_0 = 1.0$  for all plots.

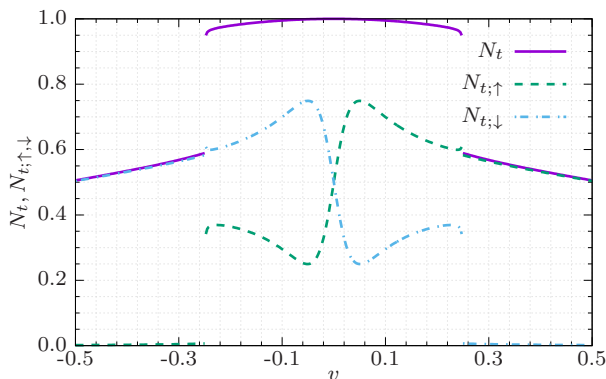


Figure 7. Amount of transported atomic matterwave for different transporting velocities. The violet solid line represents the total amount of transported matterwave  $N_t$  defined in equation (15). The green dashed and cyan dash-dotted lines represent the amount of spin- $\uparrow$  and spin- $\downarrow$  components,  $N_{t;\uparrow}$  and  $N_{t;\downarrow}$  defined in equation (14). An abrupt dropping of the amount of transported matterwave happens around  $v \approx \pm 0.25$  which is the critical velocity for the disappearing of the excited state transporting channel. The parameters used are  $k_c = 1.0$ ,  $\Omega = 0.2$ ,  $V_0 = 1.0$ .

lead to very different transporting properties of the delta-potential wells moving with different velocities.

#### IV. TRANSPORTATION

When the delta-potential well moves at a small velocity (moving induced detuning fulfills  $|\Delta| = 2k_c|v| < |\Delta_c|$ , with critical detuning  $|\Delta_c|$  having been shown in figure 5), both the ground state and excited state channels participate in the transporting, and interference will happen between them. As a result, an oscillation of the atomic density can be observed during the transporting process. The oscillating period is determined by the en-

ergy difference between the ground and excited states,  $T = 2\pi / (E_e - E_g)$ . In the left panel of figure 6, such an oscillation is shown for a delta-potential well with depth  $V_0 = 1.0$  moving at velocity  $v = 0.05$ . The ground state and excited state energies are  $-0.5742$ ,  $-0.4334$ , respectively. Therefore, the oscillating period is  $T \approx 44.63$  in the figure.

When the delta-potential well moves at a large velocity ( $|\Delta| = 2k_c|v| > |\Delta_c|$ ), the moving induced detuning eliminates the excited state transporting channel, the ground state channel plays the only transporting role. Without the excited state channel to interfere with, no oscillation happens in this case. For a positive direction moving potential, the ground state channel is spin- $\uparrow$  dominant, thus only the spin- $\uparrow$  component matterwave can be efficiently transported. While for a negative direction moving potential, the spin- $\downarrow$  dominant ground state channel can only efficiently transport the spin- $\downarrow$  component matterwave. This is shown in the middle and right panels in figure 6.

We also examined the relationship between transporting efficiency and moving velocity of the delta-potential well. The total transported atom number  $N_t$ , and atom number of each spin component  $N_{t;\uparrow,\downarrow}$  are plotted as a function of the potential moving velocity  $v$  in figure 7. In the figure, below the critical velocity ( $|v| < 0.25$ ), for a positive direction moving potential, the spin- $\uparrow$  component is a little favored; while for a negative direction moving potential, it is the spin- $\downarrow$  component favored. And the total transported atom number takes a value of nearly 1 (not less than 95%), which means that almost all the atoms can be transported in this case. However, when the velocity of the potential well exceeds the critical value ( $|v| > 0.25$ ), one of the spin components (spin- $\downarrow$  for positive, while spin- $\uparrow$  for negative direction transporting) suddenly drops to almost 0, and only the other spin component can still be transported. Except for this sudden dropping of transporting efficiency, in the figure one also notices a slowly dropping of the total

transported atom number as the transporting velocity increases. Mathematically, this is because, for a large value of  $v$ , the factor  $\exp[ivx]$  in equation (13) contributes a fast oscillation, which will reduce the transported matterwave amplitude. Physically, this can be explained by the fact that a faster moving of the potential tends to excite more atoms out of the trapping well.

At last, we also point out that here the moving of the delta-potential is switched on abruptly. However, one can also discuss the case of adiabatically switching on. In such a case, according to the adiabatical theorem [73], the atoms will adiabatically follow the ground state of the moving potential (we assume the atoms are initially prepared in the ground state). And as we have already demonstrated the dependence of ground state spin polarization on potential moving velocity in section III, therefore the unidirectional spin transport can be achieved as well.

## V. SUMMARY

In summary, we have studied the transport of SO coupled cold atomic matterwave using a moving Dirac delta-potential well. The transporting can happen in two different channels (the ground and excited bound states of the moving delta-potential well). Due to that SO coupling breaks Galilean invariance, the transport shows a

prominent unidirectional property. For small moving velocity, both the ground state and excited state channels contribute to the transportation, and the two spin components can both be efficiently transported, where spin- $\uparrow$  (spin- $\downarrow$ ) is a little favored for a positive (negative) direction transport. And under such a case, the interference between the ground state and excited state channels will cause an oscillation of the transported matterwave density. When the moving velocity exceeds a critical value, the excited state transporting channel disappears, only one spin component of the matterwave can be efficiently transported through the ground state channel. Positive direction moving delta-potential well only efficiently transports spin- $\uparrow$  component, while negative direction moving potential well only efficiently transports spin- $\downarrow$  component. The critical moving velocity is also identified in the paper. Note that some experimentally realizable potentials [64, 65, 74, 75] can be modeled by delta-function, the phenomena reported here are expected to be observed experimentally.

## ACKNOWLEDGMENTS

This work is supported by National Natural Science Foundation of China (Grant Nos. 11904063, 11847059 and 11374003).

- 
- [1] T. L. Gustavson, A. P. Chikkatur, A. E. Leanhardt, A. Görlitz, S. Gupta, D. E. Pritchard, and W. Ketterle, Transport of Bose-Einstein Condensates with optical tweezers, *Phys. Rev. Lett.* **88**, 020401 (2001).
  - [2] M. Greiner, I. Bloch, T. W. Hänsch, and T. Esslinger, Magnetic transport of trapped cold atoms over a large distance, *Phys. Rev. A* **63**, 031401 (2001).
  - [3] J. Goldwin, S. Inouye, M. L. Olsen, B. Newman, B. D. DePaola, and D. S. Jin, Measurement of the interaction strength in a Bose-Fermi mixture with Rb87 and K40, *Phys. Rev. A* **70**, 021601 (2004).
  - [4] J. A. Sauer, K. M. Fortier, M. S. Chang, C. D. Hamley, and M. S. Chapman, Cavity QED with optically transported atoms, *Phys. Rev. A* **69**, 051804 (2004).
  - [5] F. Brennecke, T. Donner, S. Ritter, T. Bourdel, M. Köhl, and T. Esslinger, Cavity QED with a Bose-Einstein condensate, *Nature* **450**, 268 (2007).
  - [6] Y. Colombe, T. Steinmetz, G. Dubois, F. Linke, D. Hunger, and J. Reichel, Strong atom-field coupling for Bose-Einstein condensates in an optical cavity on a chip, *Nature* **450**, 272 (2007).
  - [7] R. Culver, A. Lampis, B. Megyeri, K. Pahwa, L. Mudarikwa, M. Holynski, P. W. Courteille, and J. Goldwin, Collective strong coupling of cold potassium atoms in a ring cavity, *New J. Phys.* **18**, 113043 (2016).
  - [8] Y. Jiang, Y. Mei, Y. Zou, Y. Zuo, and S. Du, Efficiently loading cold atomic ensemble into an optical cavity with high optical depth, in *Conf. Lasers Electro-Optics (OSA, Washington, D.C., 2019)*, p. [JTU2A.122](#).
  - [9] W. Bowden, R. Hobson, I. R. Hill, A. Vianello, M. Schioppo, A. Silva, H. S. Margolis, P. E. G. Baird, and P. Gill, A pyramid MOT with integrated optical cavities as a cold atom platform for an optical lattice clock, *Sci. Rep.* **9**, 11704 (2019).
  - [10] M. Bajcsy, S. Hofferberth, V. Balic, T. Peyronel, M. Hafezi, A. S. Zibrov, V. Vuletic, and M. D. Lukin, Efficient all-optical switching using slow light within a hollow fiber, *Phys. Rev. Lett.* **102**, 203902 (2009).
  - [11] S. Vorrath, S. A. Möller, P. Windpassinger, K. Bongs, and K. Sengstock, Efficient guiding of cold atoms through a photonic band gap fiber, *New J. Phys.* **12**, 123015 (2010).
  - [12] M. Bajcsy, S. Hofferberth, T. Peyronel, V. Balic, Q. Liang, A. S. Zibrov, V. Vuletic, and M. D. Lukin, Laser-cooled atoms inside a hollow-core photonic-crystal fiber, *Phys. Rev. A* **83**, 063830 (2011).
  - [13] A. P. Hilton, C. Perrella, F. Benabid, B. M. Sparkes, A. N. Luiten, and P. S. Light, High-efficiency cold-atom transport into a waveguide trap, *Phys. Rev. Appl.* **10**, 044034 (2018).
  - [14] T. Yoon and M. Bajcsy, Laser-cooled cesium atoms confined with a magic-wavelength dipole trap inside a hollow-core photonic-bandgap fiber, *Phys. Rev. A* **99**, 023415 (2019).
  - [15] H. Ritsch, P. Domokos, F. Brennecke, and T. Esslinger, Cold atoms in cavity-generated dynamical optical potentials, *Rev. Mod. Phys.* **85**, 553 (2013).

- [16] L. Zhou, K. Zhang, G. Dong, and W. Zhang, Cavity quantum optics with Bose-Einstein condensates, in *Annual review of cold atoms and molecules* (World Scientific, 2013), pp. 377 - 414.
- [17] M. Adnan, Experimental platform towards in-fibre atom optics and laser cooling, Ph.D. thesis, *Université de Limoges*, 2017.
- [18] M. Arndt, A. Ekers, W. von Klitzing, and H. Ulbricht, Focus on modern frontiers of matter wave optics and interferometry, *New J. Phys.* **14**, 125006 (2012).
- [19] S. Eckel, F. Jendrzejewski, A. Kumar, C. J. Lobb, and G. K. Campbell, Interferometric measurement of the current-phase relationship of a superfluid weak link, *Phys. Rev. X* **4**, 031052 (2014).
- [20] M. Xin, W. S. Leong, Z. Chen, and S.-Y. Lan, An atom interferometer inside a hollow-core photonic crystal fiber, *Sci. Adv.* **4**, e1701723 (2018).
- [21] C. Ryu, P. W. Blackburn, A. A. Blinova, and M. G. Boshier, Experimental realization of Josephson junctions for an atom SQUID, *Phys. Rev. Lett.* **111**, 205301 (2013).
- [22] C. Ryu and M. G. Boshier, Integrated coherent matter wave circuits, *New J. Phys.* **17**, 092002 (2015).
- [23] A. Li, S. Eckel, B. Eller, K. E. Warren, C. W. Clark, and M. Edwards, Superfluid transport dynamics in a capacitive atomtronic circuit, *Phys. Rev. A* **94**, 023626 (2016).
- [24] L. Amico, G. Birkl, M. Boshier, and L.-C. Kwek, Focus on atomtronics-enabled quantum technologies, *New J. Phys.* **19**, 020201 (2017).
- [25] A. P. Chikkatur, Y. Shin, A. E. Leanhardt, D. Kielpinski, E. Tsikata, T. L. Gustavson, D. E. Pritchard, and W. Ketterle, A continuous source of Bose-Einstein condensed atoms, *Science* **296**, 2193 (2002).
- [26] T. Lahaye, G. Reinaudi, Z. Wang, A. Couvert, and D. Guéry-Odelin, Transport of atom packets in a train of Ioffe-Pritchard traps, *Phys. Rev. A* **74**, 033622 (2006).
- [27] W. Guerin, J.-F. Riou, J. P. Gaebler, V. Josse, P. Bouyer, and A. Aspect, Guided quasicontinuous atom laser, *Phys. Rev. Lett.* **97**, 200402 (2006).
- [28] M. Kasevich, D. S. Weiss, E. Riis, K. Moler, S. Kasapi, and S. Chu, Atomic velocity selection using stimulated Raman transitions, *Phys. Rev. Lett.* **66**, 2297 (1991).
- [29] K. Gibble and S. Chu, Laser-cooled Cs frequency standard and a measurement of the frequency shift due to ultracold collisions, *Phys. Rev. Lett.* **70**, 1771 (1993).
- [30] M. J. Renn, D. Montgomery, O. Vdovin, D. Z. Anderson, C. E. Wieman, and E. A. Cornell, Laser-guided atoms in hollow-core optical fibers, *Phys. Rev. Lett.* **75**, 3253 (1995).
- [31] H. Ito, T. Nakata, K. Sakaki, M. Ohtsu, K. I. Lee, and W. Jhe, Laser spectroscopy of atoms guided by evanescent waves in micron-sized hollow optical fibers, *Phys. Rev. Lett.* **76**, 4500 (1996).
- [32] D. Müller, D. Z. Anderson, R. J. Grow, P. D. D. Schwindt, and E. A. Cornell, Guiding neutral atoms around curves with lithographically patterned current-carrying wires, *Phys. Rev. Lett.* **83**, 5194 (1999).
- [33] J. Denschlag, D. Cassettari, and J. Schmiedmayer, Guiding neutral atoms with a wire, *Phys. Rev. Lett.* **82**, 2014 (1999).
- [34] M. Key, I. G. Hughes, W. Rooijakkers, B. E. Sauer, E. A. Hinds, D. J. Richardson, and P. G. Kazansky, Propagation of cold atoms along a miniature magnetic guide, *Phys. Rev. Lett.* **84**, 1371 (2000).
- [35] K. E. Strecker, G. B. Partridge, A. G. Truscott, and R. G. Hulet, Formation and propagation of matter-wave soliton trains, *Nature* **417**, 150 (2002).
- [36] A. E. Leanhardt, A. P. Chikkatur, D. Kielpinski, Y. Shin, T. L. Gustavson, W. Ketterle, and D. E. Pritchard, Propagation of Bose-Einstein condensates in a magnetic waveguide, *Phys. Rev. Lett.* **89**, 040401 (2002).
- [37] L. Plaja and L. Santos, Expansion of a Bose-Einstein condensate in an atomic waveguide, *Phys. Rev. A* **65**, 035602 (2002).
- [38] S. Gupta, K. W. Murch, K. L. Moore, T. P. Purdy, and D. M. Stamper-Kurn, Bose-Einstein condensation in a circular waveguide, *Phys. Rev. Lett.* **95**, 143201 (2005).
- [39] J. Bravo-Abad, M. Ibanescu, J. D. Joannopoulos, and M. Soljačić, Photonic crystal optical waveguides for on-chip Bose-Einstein condensates, *Phys. Rev. A* **74**, 053619 (2006).
- [40] A. L. Marchant, T. P. Billam, T. P. Wiles, M. M. H. Yu, S. A. Gardiner, and S. L. Cornish, Controlled formation and reflection of a bright solitary matter-wave, *Nat. Commun.* **4**, 1865 (2013).
- [41] W. Hänsel, J. Reichel, P. Hommelhoff, and T. W. Hänsch, Magnetic conveyor belt for transporting and merging trapped atom clouds, *Phys. Rev. Lett.* **86**, 608 (2001).
- [42] S. Schmid, G. Thalhammer, K. Winkler, F. Lang, and J. H. Denschlag, Long distance transport of ultracold atoms using a 1D optical lattice, *New J. Phys.* **8**, 159 (2006).
- [43] A. Couvert, T. Kawalec, G. Reinaudi, and D. Guéry-Odelin, Optimal transport of ultracold atoms in the non-adiabatic regime, *Europhys. Lett.* **83**, 13001 (2008).
- [44] A. Alberti, V. V. Ivanov, G. M. Tino, and G. Ferrari, Engineering the quantum transport of atomic wavefunctions over macroscopic distances, *Nat. Phys.* **5**, 547 (2009).
- [45] R. Roy, P. C. Condylis, V. Prakash, D. Sahagun, and B. Hessmo, A minimalistic and optimized conveyor belt for neutral atoms, *Sci. Rep.* **7**, 13660 (2017).
- [46] K. O. Chong, J.-R. Kim, J. Kim, S. Yoon, S. Kang, and K. An, Observation of a non-equilibrium steady state of cold atoms in a moving optical lattice, *Commun. Phys.* **1**, 25 (2018).
- [47] K. Zhou and Z. Zhang, Opposite effect of spin-orbit coupling on condensation and superfluidity, *Phys. Rev. Lett.* **108**, 025301 (2012).
- [48] J. P. Vyasankere and V. B. Shenoy, Collective excitations, emergent Galilean invariance, and boson-boson interactions across the BCS-BEC crossover induced by a synthetic Rashba spin-orbit coupling, *Phys. Rev. A* **86**, 053617 (2012).
- [49] Y. Zhang, M. E. Mossman, T. Busch, P. Engels, and C. Zhang, Properties of spin-orbit-coupled Bose-Einstein condensates, *Front. Phys.* **11**, 118103 (2016).
- [50] Q. Zhu, C. Zhang, and B. Wu, Exotic superfluidity in spin-orbit coupled Bose-Einstein condensates, *Europhys. Lett.* **100**, 50003 (2012).
- [51] J.-Y. Zhang, S.-C. Ji, Z. Chen, L. Zhang, Z.-D. Du, B. Yan, G.-S. Pan, B. Zhao, Y.-J. Deng, H. Zhai, S. Chen, and J.-W. Pan, Collective dipole oscillations of a spin-orbit coupled Bose-Einstein condensate, *Phys. Rev. Lett.* **109**, 115301 (2012).
- [52] Y. Li, G. I. Martone, and S. Stringari, Sum rules, dipole oscillation and spin polarizability of a spin-orbit coupled quantum gas, *Europhys. Lett.* **99**, 56008 (2012).
- [53] Y. Xu, Y. Zhang, and B. Wu, Bright solitons in spin-orbit-coupled Bose-Einstein condensates,



- Phys. Rev. A* **87**, 013614 (2013).
- [54] C. Hamner, Y. Zhang, M. A. Khamehchi, M. J. Davis, and P. Engels, Spin-orbit-coupled Bose-Einstein condensates in a one-dimensional optical lattice, *Phys. Rev. Lett.* **114**, 070401 (2015).
- [55] Y.-C. Zhang, Z.-Q. Yu, T. K. Ng, S. Zhang, L. Pitaevskii, and S. Stringari, Superfluid density of a spin-orbit-coupled Bose gas, *Phys. Rev. A* **94**, 033635 (2016).
- [56] M. E. Mossman, J. Hou, X.-W. Luo, C. Zhang, and P. Engels, Experimental realization of a non-magnetic one-way spin switch, *Nat. Commun.* **10**, 3381 (2019).
- [57] C.-H. Li, C. Qu, R. J. Niffenegger, S.-J. Wang, M. He, D. B. Blasing, A. J. Olson, C. H. Greene, Y. Lyanda-Geller, Q. Zhou, C. Zhang, and Y. P. Chen, Spin current generation and relaxation in a quenched spin-orbit-coupled Bose-Einstein condensate, *Nat. Commun.* **10**, 375 (2019).
- [58] L. W. Cheuk, A. T. Sommer, Z. Hadzibabic, T. Yefsah, W. S. Bakr, and M. W. Zwierlein, Spin-Injection Spectroscopy of a Spin-Orbit Coupled Fermi Gas, *Phys. Rev. Lett.* **109**, 095302 (2012).
- [59] J. Lan, W. Yu, R. Wu, and J. Xiao, Spin-wave diode, *Phys. Rev. X* **5**, 041049 (2015).
- [60] Y.-J. Zhao, D. Yu, L. Zhuang, X. Gao, and W.-M. Liu, Tunable spinful matter wave valve, *Sci. Rep.* **9**, 8653 (2019).
- [61] M. Lebrat, S. Häusler, P. Fabritius, D. Husmann, L. Corman, and T. Esslinger, Quantized conductance through a spin-selective atomic point contact, *Phys. Rev. Lett.* **123**, 193605 (2019).
- [62] L. Corman, P. Fabritius, S. Häusler, J. Mohan, L. H. Dogra, D. Husmann, M. Lebrat, and T. Esslinger, Quantized conductance through a dissipative atomic point contact, *Phys. Rev. A* **100**, 053605 (2019).
- [63] Y.-J. Lin, K. Jimenez-Garcia, and I. B. Spielman, Spin-orbit-coupled Bose-Einstein condensates, *Nature* **471**, 83 (2011).
- [64] H. Uncu, D. Tarhan, E. Demiralp, and Ö. E. Müstecaplıoğlu, Bose-Einstein condensate in a harmonic trap decorated with Dirac  $\delta$  functions, *Phys. Rev. A* **76**, 013618 (2007).
- [65] M. C. Garrett, A. Ratnapala, E. D. van Ooijen, C. J. Vale, K. Weegink, S. K. Schnelle, O. Vainio, N. R. Heckenberg, H. Rubinsztein-Dunlop, and M. J. Davis, Growth dynamics of a Bose-Einstein condensate in a dimple trap without cooling, *Phys. Rev. A* **83**, 013630 (2011).
- [66] C. Chin, R. Grimm, P. Julienne, and E. Tiesinga, Feshbach resonances in ultracold gases, *Rev. Mod. Phys.* **82**, 1225 (2010).
- [67] E. Timmermans, P. Tommasini, M. Hussein, and A. Kerman, Feshbach resonances in atomic Bose-Einstein condensates, *Phys. Rep.* **315**, 199 (1999).
- [68] E. Granot and A. Marchewka, Quantum particle displacement by a moving localized potential trap, *Europhys. Lett.* **86**, 20007 (2009).
- [69] E. Sonkin, B. A. Malomed, E. Granot, and A. Marchewka, Trapping of quantum particles and light beams by switchable potential wells, *Phys. Rev. A* **82**, 033419 (2010).
- [70] J. Qin, R. Zheng, and L. Zhou, Bound states of spin-orbit coupled cold atoms in a Dirac delta-function potential, *J. Phys. B At. Mol. Opt. Phys.* **53**, 125301 (2020).
- [71] V. A. Sablikov and Y. Y. Tkach, Evanescent states in two-dimensional electron systems with spin-orbit interaction and spin-dependent transmission through a barrier, *Phys. Rev. B* **76**, 245321 (2007).
- [72] L. Zhou, J.-L. Qin, Z. Lan, G. Dong, and W. Zhang, Goos-Hänchen shifts in spin-orbit-coupled cold atoms, *Phys. Rev. A* **91**, 031603(R) (2015).
- [73] T. Kato, On the Adiabatic Theorem of Quantum Mechanics, *J. Phys. Soc. Japan* **5**, 435 (1950).
- [74] M. Łacki, M. A. Baranov, H. Pichler, and P. Zoller, Nanoscale “dark state” optical potentials for cold atoms, *Phys. Rev. Lett.* **117**, 233001 (2016).
- [75] Y. Wang, S. Subhankar, P. Bienias, M. Łacki, T.-C. Tsui, M. A. Baranov, A. V. Gorshkov, P. Zoller, J. V. Porto, and S. L. Rolston, Dark state optical lattice with a subwavelength spatial structure, *Phys. Rev. Lett.* **120**, 083601 (2018).